Gas-Liquid Flow on Smooth and Textured Inclined Planes

J.J. Cooke, S. Gu, L.M. Armstrong and K.H. Luo

Abstract—Carbon Capture & Storage (CCS) is one of the various methods that can be used to reduce the carbon footprint of the energy sector. This paper focuses on the absorption of CO2 from flue gas using packed columns, whose efficiency is highly dependent on the structure of the liquid films within the column. To study the characteristics of liquid films a CFD solver, OpenFOAM is utilised to solve two-phase, isothermal film flow using the volume-of-fluid (VOF) method. The model was validated using existing experimental data and the Nusselt theory. It was found that smaller plate inclination angles, with respect to the horizontal plane, resulted in larger wetted areas on smooth plates. However, only a slight improvement in the wetted area was observed. Simulations were also performed using a ridged plate and it was observed that these surface textures significantly increase the wetted area of the plate. This was mainly attributed to the channelling effect of the ridges, which helped to oppose the surface tension forces trying to minimise the surface area. Rivulet formations on the ridged plate were also flattened out and spread across a larger proportion of the plate width.

Keywords—CCS, liquid film flow, packed columns, wetted area

I. INTRODUCTION

LIQUID films are an important feature throughout many areas of engineering, ranging from falling film microreactors [1], [2] to Carbon Capture & Storage (CCS). CCS using packed columns involves the capture of CO2 using an amine solution, usually monoethanolamine (MEA). Aqueous MEA undergoes a reversible reaction with CO2, whereby the chemical equilibrium and rate of reaction are dependent upon many factors, including the surface film structure. CO2 is removed from exhaust gases in the absorber, where cooled MEA flows counter-current to the gas flow. The amine solution is then heated in order to shift the chemical equilibrium of the system. CO2 is subsequently removed from the solution in a stripper using a counter-current flow of steam [3]. The regenerated MEA is cooled before re-entering the cycle.

Packed columns are used to enhance heat and mass transfer by providing large gas-liquid interfacial areas. Structured packings usually consist of layers of corrugated metal sheets orientated with various inclination angles. This arrangement helps to promote gas-liquid mixing within the packing, increasing absorption rates.

The major difficulty that arises when modelling carbon capture through packed columns is the large range of spatial scales that exist throughout the process. To accurately model the whole system, near wall effects must be accounted for, requiring detailed modelling of the liquid films. However, absorbers and strippers have characteristic sizes on the scale of meters and so even with the current computing power it is impossible to resolve all of these spatial scales simultaneously during a numerical simulation. Furthermore, the inclusion of reaction kinetics into the model introduces additional complexity.

To overcome these difficulties the method proposed by Raynal and Royon-Lebeaud [4] involves segmenting the problem into three ranges of spatial scales; the micro-scale (liquid films on the packing), meso-scale (element of packing material) and macro-scale (full absorber). Following this framework, results from each of the scales are input into the subsequent larger scales.

This investigation involved simulating the micro-scale. The intricate fluid flow behaviour throughout packings was simplified down to film flow over an inclined plane. By reducing the number of parameters and complexity of the problem in this way, a detailed analysis of the film flow was performed. The findings in this paper could be used as the basis for an optimisation study in order to determine the optimum packing structure for CCS.

It is important to determine the fluid dynamics of liquid films because the efficiency of CO2 absorption is closely related to the structure of the liquid films within the packing materials. Liquid films can exhibit a range of flow regimes, including full film, rivulet and droplet flow. The formation of these features is dependent upon various flow parameters, such as liquid flow rate, plate surface texture, plate geometry etc.

Previous experimental studies have been undertaken to investigate the effect of surface texture on liquid-side mass transfer during liquid film flows [5]. It was found that a textured surface, typically found in commercial packing materials, can increase the mass-side transfer by as much as 80% in comparison to a smooth plate [5]. Three-dimensional CFD investigations of heat and mass transfer have been performed [6]–[8]. However, these papers do not examine the effect of surface texture on the heat and mass transfer, exclusively investigating smooth corrugated packing materials.

Haroun *et al.* [9] performed direct numerical simulations of gas-liquid flow on two-dimensional structured surfaces using a modified volume-of-fluid (VOF) approach. Szulczewska *et al.* [10] also used the VOF method to study liquid film flow using a two-dimensional approach. They studied the dependency of the interfacial area on the gas and liquid flow rates during counter-current flow. However, liquid films can exhibit highly three-dimensional structures, such as rivulets, and these can

J.J. Cooke, L.M. Armstrong and K.H. Luo are with the Energy Technology Research Group, School of Engineering Sciences, University of Southampton, Southampton SO17 1BJ, United Kingdom

S. Gu is with the School of Engineering, Cranfield University, Cranfield, Bedfordshire MK43 0AL, United Kingdom (Tel: +441234 755277; Fax: +441234 754685; Email address: s.gu@cranfield.ac.uk)

not be observed when using a two-dimensional model.

There have been many papers in the literature specifically looking at liquid films in an effort to understand the hydro-dynamic behaviour of packed columns and other gas-liquid contactors at the micro-scale. Lan *et al.* [11] used a combined experimental and three-dimensional, isothermal CFD approach to study thin film flow on inclined planes. They focused on the effects that surface tension, contact angle, film flow rate and inclination angle had on the film velocity, width and thickness. However, this investigation did not specifically focus on liquid films within packed columns and so surface texture was not taken into account.

The analysis of counter-current gas-liquid flow at the micro-scale is of particular importance in the understanding of the processes involved in packed columns. Counter-current gas flow has been observed to increase the thickness and fluctuation of liquid films [12]. Furthermore, thin films may be susceptible to break-up and hence, thicker films are more suitable when this flow arrangement is used [13].

Micro-scale surface texture on packed columns has been found to have a large effect on the structure of liquid films [13]. Valluri *et al.* [14] developed an analytical model for film flow over sinusoidal and doubly sinusoidal surfaces at moderate Reynolds numbers. A CFD approach was used to assess the viability of the model. The analytical model was shown to provide good correlation with the CFD results for $Re_l < 30$. However, this approach was limited to a two-dimensional analysis and as mentioned previously, liquid films can exhibit behaviour such as rivulets which can only be fully resolved by three-dimensional models or simulations.

Full films provide the greatest efficiency because the large surface area is conducive to CO2 absorption. The formation of rivulets, or any other phenomena which reduces the wetted area of the packing, hinders heat and mass transfer. These three-dimensional phenomena have been successfully modelled using the VOF approach and it has been shown that the structure of a film is highly dependent upon the geometry and the choice of boundary conditions during numerical simulations [15], [16].

Following on from this, Iso and Chen [17] examined the transition behaviour between the different flow regimes exhibited on inclined plates. Three-dimensional, isothermal VOF simulations were used to analyse the transition between rivulet flow and full film flow. It was observed that a hysteresis phenomena occurred, depending on whether the liquid flow rate was increasing or decreasing, suggesting that the flow is also affected by past flow patterns. This emphasises the importance of performing time-dependent simulations to accurately resolve the film flow features.

Iso and Chen [17] also showed that a particular surface texture on the packing material was able to increase the wetted area, which would enhance heat and mass transfer. However, it is also important to examine the negative effects of surface texture, which may hinder heat and mass transfer. For example, sinusoidal structures of certain amplitudes have been shown to cause recirculation in the film, resulting in regions of stagnant fluid [13], [14]. These regions will reduce the efficiency of CO2 absorption within packed columns.

This investigation used the CFD solver, OpenFOAM [18], [19] to study three-dimensional, two-phase, isothermal film flow using the VOF method. The first section of this paper looks at gravity driven film flow over smooth surfaces. The results are validated by comparison with experimental data from the literature and the Nusselt theory. Multiple inclination angles are investigated to determine the effect of the inclination angle on the wetted area. The second part of this paper details the results of film flow over a plate with unique surface texture. Comparison are made between the smooth and textured plate, in terms of wetted area, interfacial velocities and thickness of the liquid films.

II. NUMERICAL METHODOLOGY

A. Modelling and Governing Equations

This investigation used the CFD software, OpenFOAM [18], [19], a set of c++ libraries used to solve fluid flow problems. In particular, the solver interFOAM enabled the solution of multiphase, isothermal flow to be calculated, where reactions were neglected.

The flow through packed columns is highly complex due to the multiphase, multiscale and reactive nature of the system. At present, this can only be accomplished by some form of simplification or decomposition of scales [4]. This investigation focuses on the micro-scale, where liquid film flow within packed columns can be approximated by flow down an inclined plane. Reaction kinetics were neglected in order to further simplify the approach. These simplifications allowed film flow to be studied in detail, examining the effects of variation of parameters and of surface texture on the wetted area and other characteristics of the flow.

The VOF method [20] used in interFOAM can be used to solve multiphase flow of incompressible, isothermal, immiscible fluids. A single momentum equation is solved for the mixture and the fluid properties of each phase are combined to form fluid properties of the mixture. The interface between the phases is resolved using an interface capturing technique. This is achieved by solving a transport equation for the volume fraction.

The volume fraction, α_i is used to determine the volume of phases within each computational cell. The total volume fraction for a cell is defined to be 1 and therefore, the volume fraction for each phase can lie in the range $0 \leq \alpha_i \leq 1$. If a cell is completely filled with the ith phase then $\alpha_i = 1$ and if a cell is completely devoid of the ith phase then $\alpha_i = 0$. The interface region can be constructed using the values of α_i in the cells across the domain. For a two-phase system, as is the case in this paper, the volume fraction is determined for one phase and the other phase is tracked trivially, $\alpha_2 = 1 - \alpha_1$.

Fluid properties such as the density, ρ and the dynamic viscosity, μ are defined in each cell as a function of the volume fraction and are given by:

$$\rho = \alpha_1 \rho_1 + (1 - \alpha_1)\rho_2, \tag{1}$$

$$\mu = \alpha_1 \mu_1 + (1 - \alpha_1)\mu_2, \tag{2}$$

where the subscripts relate to the individual properties of each phase.

The volume fractions throughout the domain can be determined by solving transport equations for α_i. In a two-phase fluid a single transport equation for α_1 is required, since α_2 can be determined trivially. The transport equation for α_1 used in the interFOAM solver is defined by [21]:

$$\frac{\partial \alpha_1}{\partial t} + \nabla.(\overrightarrow{v}\alpha_1) + \nabla.(\overrightarrow{v_r}\alpha_1(1-\alpha_1)) = 0, \qquad (3)$$

where $\overrightarrow{v_r}$ is a suitable velocity field selected to compress the interfacial region [22]. Equation 3 is the continuity equation for α_1, with the notable addition of the 3rd term. As described by Rusche [21], this is an artificial compression term used to provide interface compression without the use of a compressive differencing scheme, with the advantage that the solution for α_1 is bounded between 0 and 1, as required by the definition of volume fraction. Due to the form of this extra term it is only significant in the interfacial region, where it is required and hence, has little effect on the solution throughout the rest of the domain.

Due to the low liquid film Reynolds numbers encountered in the simulations in this paper ($Re_l < 230$) the flow can be considered laminar. In the laminar regime the momentum equation is given by:

$$\frac{\partial(\rho\overrightarrow{v})}{\partial t} + \nabla.(\rho\overrightarrow{v}\overrightarrow{v}) - \nabla.\mu\nabla\overrightarrow{v} = -\nabla p + \rho\overrightarrow{g} + \overrightarrow{F_s}. \quad (4)$$

The contribution to the balance of momentum from surface tension, $\overrightarrow{F_s}$ is modelled using the continuum surface force model (CSF) model [23] and is given by:

$$\overrightarrow{F_s} = \sigma k(\overrightarrow{x})\overrightarrow{n}, \qquad (5)$$

where σ is the surface tension, $\overrightarrow{n}$ (see equation 6 and 8) is the unit normal vector to the interface and $k(\overrightarrow{x})$ (see equation 7) is the curvature of the interface.

$$\overrightarrow{n} = \frac{\nabla\alpha}{|\nabla\alpha|}, \qquad (6)$$

$$k(\overrightarrow{x}) = \nabla.\overrightarrow{n}. \qquad (7)$$

In cells adjacent to a wall boundary the definition of the unit normal vector is adjusted in order to take account of the liquid contact angle. The method in this paper used a constant wall contact angle, θ_w and the unit normal vector is defined as [13]:

$$\overrightarrow{n} = \overrightarrow{n_w}cos(\theta_w) + \overrightarrow{m_w}sin(\theta_w), \qquad (8)$$

where $\overrightarrow{n_w}$ is the unit vector normal to the wall and $\overrightarrow{m_w}$ is the unit vector tangential to the wall.

An important non-dimensional parameter used in this investigation was the liquid film Reynolds number, Re_l, defined by [17]:

$$Re_l = \frac{\rho_l \cdot V_l \cdot \delta}{\mu_l}, \qquad (9)$$

where V_l is the average liquid film velocity defined as

$$V_l = \frac{Q_l}{\delta \cdot w}. \qquad (10)$$

Q_l is the volumetric flow rate of the liquid and w is the width of the film on the plate, which is approximated as the full
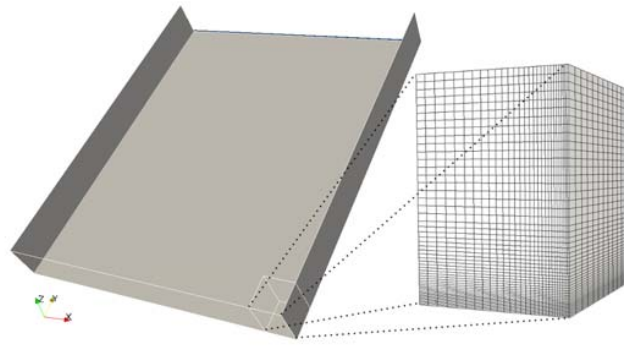

Fig. 1. Computational domain and mesh for smooth plate

width of the plate during these simulations. The liquid film thickness, δ is given by:

$$\delta = \left[\frac{3 \cdot \mu_l \cdot Q_l}{(\rho_l - \rho_g) \cdot g \cdot sin\theta \cdot w}\right]^{\frac{1}{3}}, \qquad (11)$$

where θ is the plate inclination angle and the subscripts, l and g refer to the liquid and gas phases respectively.

The specific wetted area of a plate, a is calculated as the ratio of the wetted area to the total area of the plate,

$$a = \frac{A_w}{A_t}. \qquad (12)$$

Hence, the value of the specific wetted area lies in the range $0 < a < 1$, where $a = 1$ represents full film flow.

B. Computational Domain

The computational domains in this paper are based on an inclined steel plate [15]–[17], representative of a small section of packing material. The smooth plate has dimensions of 0.06 m $\times$ 0.05 m (width$\times$height). The total depth of the domain was 0.007 m and steel walls were placed at the sides of the plate. The liquid inlet has a depth of 0.4 mm across the width of the plate [15]–[17]. The investigation used two different domains, one smooth plate and one with surface texture. A diagram of the smooth plate is shown in Fig. 1. The smooth plate was meshed with 1.0 million cells, which was selected after a grid independence study had been performed (see appendix A-A).

The textured plate maintained the same overall dimensions as the smooth plate and consisted of ridges running along the 0.06 m length of the plate. The ridges were 0.2 mm high, 0.4 mm wide and spaced 0.8 mm apart from each other. These dimensions were chosen to be of a similar scale to the liquid film thickness, so that their addition would have a noticeable effect on the film flow. A diagram of the textured plate is shown in Fig. 2. The grid for the textured plate consisted of 2.5 million cells, selected after a grid independence study (see appendix A-B).

All computational grids in this paper use structured non-uniform hexahedral cells, so as to maintain a high degree of accuracy whilst using the VOF method. This approach resulted
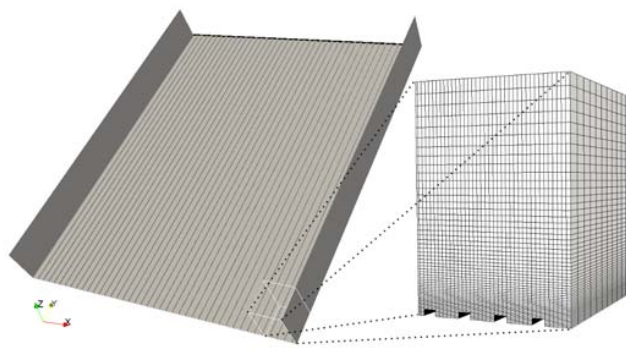
Fig. 2.   Computational domain and mesh for textured plate

Fig. 3.   The specific wetted area against Re_l

in a rather large number of cells for the textured plate domain, considering the level of refinement required around the ridges to fully resolve the flow. However, it was important to maintain the level of accuracy achieved by using structured grids.

Due to the increased surface area of the textured plate it was important to introduce a correction to the specific wetted area calculation, so that direct comparisons could be made between the smooth and textured plate. The correction involved neglecting plate surfaces that were perpendicular to the film surface (e.g. side walls of the ridges), since inclusion of these surfaces would over-estimate the actual interfacial surface area.

C. Simulation Set-Up

The simulations were performed using various flow parameters. For the smooth plane, multiple inclination angles, θ were selected in order to determine the effect of inclination angle on the film flow. Simulations were run at angles, $\theta = 30^o$ and $\theta = 60^o$. The velocity of the liquid film at the inlet was altered to give a range of Re_l.

For the textured plate, the inclination angle was fixed at $\theta = 60^o$ for all simulations and the only varied parameter was the Re_l. The ridges on the textured plate had the effect of reducing the area of the liquid inlet and hence, the liquid flow velocity was increased in order to maintain equivalent Re_l. This allowed direct comparisons to be made between the results of the smooth and textured plates.

Simulations were conducted as time-dependent runs, stepping to steady or pseudo-steady states. All simulations were run using a variable time-step to keep the Courant number below 1.0. This resulted in time steps of the order $1 \times 10^{-5} s$. Steady state convergence was assured by monitoring the specific wetted area of the plates as a function of time.

The dynamic viscosity and density of the constituent phases were $\mu_l = 8.899 \times 10^{-4}$ Pa$\cdot$s and $\rho_l = 997$ Kg$\cdot$m^{-3} for the liquid and $\mu_g = 1.831 \times 10^{-5}$ Pa$\cdot$s and $\rho_g = 1.185$ Kg$\cdot$m^{-3} for the gas. The surface tension was set to $\sigma = 0.0728$ N$\cdot$m^{-1} and the static contact angle was set to $\theta_w = 70^o$.

As mentioned previously, the simulations were run as laminar because of the low liquid film Reynolds numbers
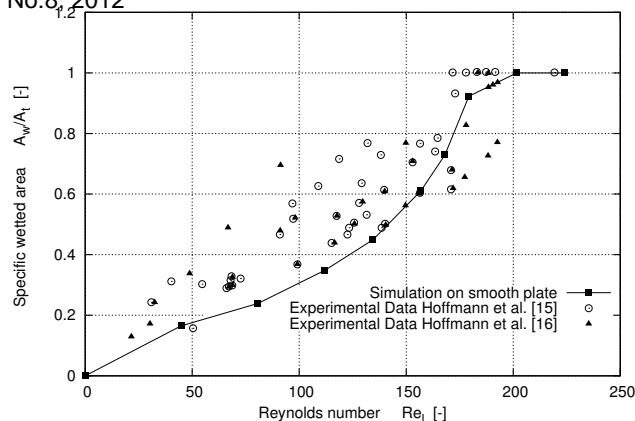
encountered, $Re_l < 230$. Counter-current gas flow was not enforced to enable validation with experimental data from the literature.

III. RESULTS AND DISCUSSION

A. Validation

Validation of the methods used in this paper were performed by comparison with data from previous studies in the literature and with the predictions of the Nusselt theory. Simulations were performed using the smooth plate with various liquid inlet velocities at an inclination angle of $\theta = 60^o$. The results are shown in Fig. 3, where the specific wetted area of the plate was plotted against Re_l. To provide comparative data, existing experimental results from the literature [15], [16] are also plotted in Fig. 3.

It is noted that the numerical method under-estimates the wetted area at lower Re_l, but is able to correctly predict the wetted area at larger Re_l. This may be due to the fact that a uniform velocity boundary condition was used at the liquid inlet. Therefore, the film would have to flow a certain distance down the plate before a full film velocity profile was established. At lower Re_l the rivulets began to form at a position close to the liquid inlet. Here, a full film velocity profile was not established and so this may have had an effect on the resulting formation of rivulets. Whereas, at higher Re_l the rivulets were formed further down the plate, where the full film velocity profile was established. Despite these uncertainties, the difference between the numerical and experimental data was minimal.

Further validation was performed by comparison of the simulated film velocity profile against the predictions of the Nusselt theory [24]. The data for the film velocity profile was extracted from a position 0.5 mm above the outlet along the centre of the plate. The central position was chosen in order to minimise the side wall effects on the velocity profile and was placed far away from the inlet to ensure that a fully developed film profile was observed. The simulation was performed at $Re_l = 224$, where a full film had developed across the whole of the plate. Fig. 4 shows the comparison between
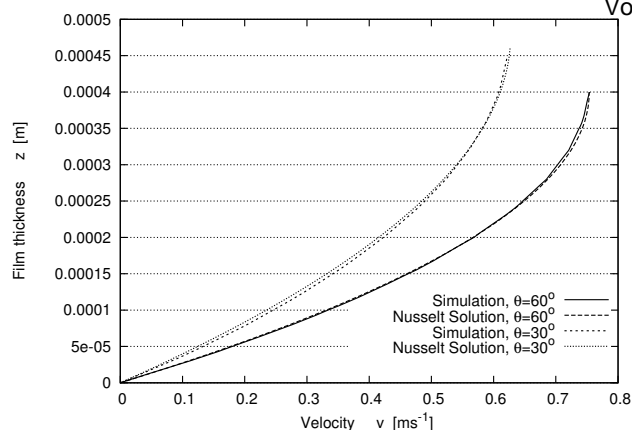
Fig. 4. Comparison of film velocity profile against the Nusselt solution at $Re_l = 224$

Fig. 5. Comparison of specific wetted area for a range of Re_l at inclination angles of 30° and 60°

the simulated results and the Nusselt theory predictions for inclination angles of $\theta = 30^o$ and $\theta = 60^o$.

Figures 3 and 4 show that the numerical methods used in this paper produced results in good correlation with previous experimental data and theoretical predictions. Therefore, it can be assumed that these methods can be used with confidence in further simulations to accurately solve for film flow on inclined planes.

B. Smooth Plate

The inclination angle of surfaces within packed columns is an important choice to make when designing packing materials. The performance of packed columns depends on the inclination angle in a number of ways. As noted by Petre *et al.* [25], shallow angles of inclination (with respect to the horizontal) result in large pressure drops when compared to steeper inclination angles. During the carbon capture process the pressure drop through the column needs to be kept to a minimum, considering that the flue gas is at a relatively low pressure. The smaller the pressure drop, the taller the column can be used, resulting in a greater volume of CO2 absorption. From a pressure drop perspective, large inclination angles are optimal. However, it is also important to examine the effect that the inclination angle has on the resulting wetted area of the packing materials.

To the best of the authors' knowledge, no previous paper has examined the effect of inclination angle on the wetted area of inclined plates across a range of Re_l. The wetted area was simulated for a range of Re_l for inclination angles of 30° and 60°. The results are plotted in Fig. 5. It can be seen that smaller inclination angles result in larger wetted areas, across the whole range of Re_l tested. This would make a positive contribution to heat and mass transfer, but a higher pressure drop would be encountered. Further investigation will need to be performed to analyse whether the advantage gained by the increased interfacial surface area is offset by the increased pressure drop.
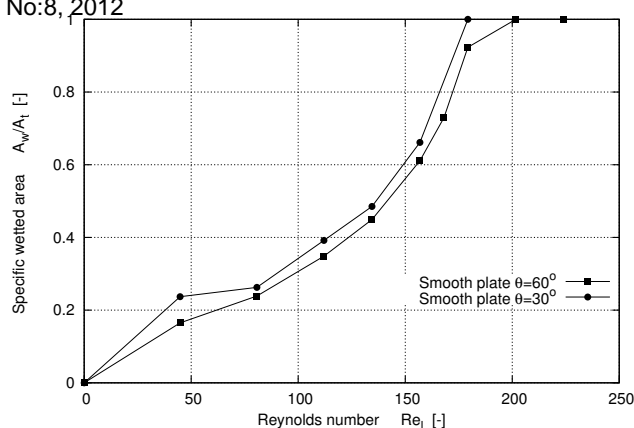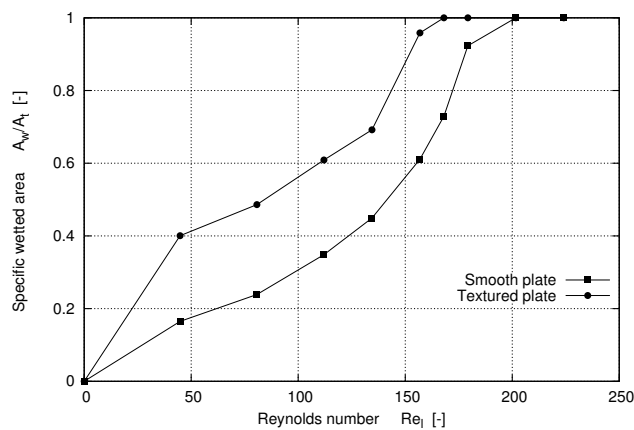

Fig. 6. Specific wetted area against Re_l for smooth and textured plate ($\theta = 60^o$)

C. Textured Plate

This section discusses the results of film flow over inclined planes with surface textures. The ridged surface of the plate was devised in order to increase the wetted area of the plate. Fig. 6 shows a comparison of the specific wetted area of the smooth plate and the ridged plate for a range of Re_l at $\theta = 60^o$. It was observed that the addition of ridges, running parallel to the flow direction, significantly increased the wetted area of the plate at all $Re_l < 200$.

At low Re_l, droplet flow is dominant and in this regime surface tension forces tend to reduce the interfacial surface area of the liquid droplets. The addition of ridges to the plate causes channelling of the flow, which reduces the surface area minimising effect of surface tension.

At mid-range Re_l, rivulet flow, induced by surface tension forces, causes a reduction in the interfacial surface area. As can be seen in Fig. 7, rivulets can form with a thickness of several times that of the preceding film flow. It can also be seen in Fig. 7 that ridges on the plate help to spread the rivulet over a much larger area across the width of the plate,
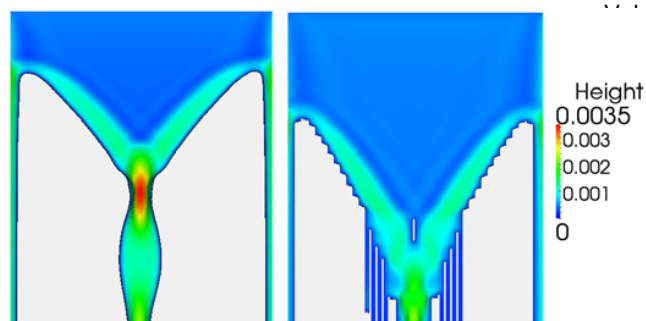
Fig. 7. Thickness of liquid film at $Re_l = 134.44$ and $\theta = 60^o$ (left: Smooth plate, right: Textured plate)

TABLE I
SPECIFIC WETTED AREA FOR SMOOTH AND TEXTURED PLATE AT $\theta = 60^o$

Re_l [-]	A_w^{smooth}/A_t [-]	$A_w^{textured}/A_t$ [-]	Increase in Wetted Area [%]
0	0	0	0
44.81	0.164787	0.400508	143.05
80.67	0.238929	0.486207	103.49
112.04	0.348422	0.608895	74.76
134.44	0.449249	0.69194	54.02
156.85	0.610955	0.958555	56.89
168.05	0.729229	1	37.13
179.26	0.923153	1	8.32
201.66	1	1	0
224.07	1	1	0

thus increasing the wetted area. Furthermore, capillary effects induced by the small size of the channels draws liquid down the plate, breaking up the leading edge of the film.

It is interesting to note that the textured surface has a much larger effect on the wetted area at the lower range of Re_l tested. Table I shows the percentage increase in the wetted area from the smooth plate to the textured plate. Therefore, if one only considers the interfacial area, the textured plate will result in increased heat and mass transfer within a packed column. However, the transfer rates are dependent upon many other factors, which have been neglected during this study, to reduce complexity. It will be important to determine the effects of these ridges on other aspects of the system. For example, these ridges may prevent the transport of MEA through the liquid film, resulting in regions of CO2-rich MEA solution near the film surface and CO2-lean MEA solution within the ridges. If MEA transport is inhibited, then the CO2 absorption rate may be reduced, cancelling out the advantages created by the increased wetted area. The exact nature of these effects is only speculative and is out of the scope of this paper. It is planned that these will be investigated in future papers, where reaction kinetics will be included in the model.

It is important to determine the effect that the ridges have on heat and mass transfer since most of the differences are seen for Re_l below 200, beyond which the inclination angle and the surface wall texture has less of an influence. However, it is crucial to remember that idealisations have been made in order to reduce the complexity of the problem. In reality, the Re_l and the film structure will depend upon many factors, such as liquid flow rate, the distribution of liquid throughout the columns, corrugation angle, inclination angle of the packing, etc. Further meso-scale simulations will need to be performed to determine the exact liquid distribution over the packing. This paper shows that the addition of ridges should improve the wetted area of full-scale packing up to a limiting Re_l. The limiting Re_l will be dependent on the specific problem being investigated and it can be defined as the point at which full film flow occurs.

Fig. 8 shows the interfacial velocity magnitude for the smooth and textured plates at $Re_l = 179.26$ and $\theta = 60^o$ and Fig. 9 shows a close-up view of the velocity vectors within this film along the plane $y = 0.02$ m. It is observed that the ridges on the plate create alternate layers of varying interfacial
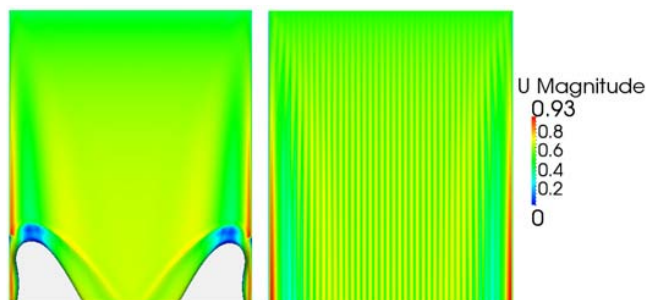

Fig. 8. Interfacial velocity contours of liquid film at $Re_l = 179.26$ and $\theta = 60^o$ (left: Smooth plate, right: Textured plate)
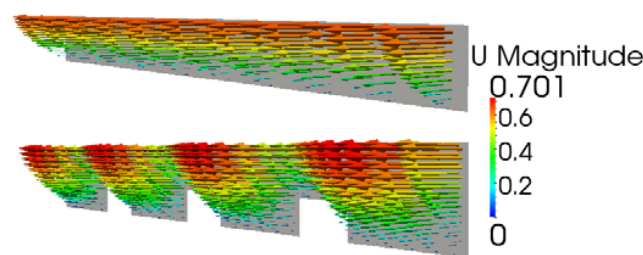

Fig. 9. Velocity vectors within the liquid film along the plane $y = 0.02$ m at $Re_l = 179.26$ and $\theta = 60^o$ (top: Smooth plate, bottom: Textured plate)

velocities along the surface of the film. This is attributed to the reduction in film thickness, due to the presence of the ridges. Fig. 9 shows that the addition of ridges along the plate does not result in regions of stagnant fluid within the channels. Furthermore, the variation in velocity throughout the film and the film surface may assist in the heat and mass transfer process, since different layers of fluid within the film move at different velocities. However, as mentioned previously, the impact of these structures on the CO2 absorption process will have to be assessed in future investigations.

Packing materials also have a corrugation angle (usually 45°) as well as an inclination angle. The corrugation angle was neglected in this paper, but it is predicted that the effect of this would be to cause liquid to accumulate at the sides of the plate. The channels on the textured packing may help to prevent such accumulation of liquid and help to produce more evenly distributed films.

Also, this paper has assumed an inlet flow across the whole width of the plate. However, in reality this may not be the case, especially well within the packed column. In the case of a point source of liquid the channels may even reduce the wetted area. This will have to be investigated further and modifications to the design could help to increase the wetted area for various inlet conditions.

IV. CONCLUSION

In this paper the VOF method was used to study isothermal liquid film flow down inclined planes. Initially, simulations were performed on a smooth plate and the effect of inclination angle on the wetted area was studied for a range of Re_l. The methods used throughout this paper were validated using existing experimental data and theoretical predictions. It was found that an decrease in the inclination angle resulted in larger wetted areas at the respective Re_l. However, the increases observed were minimal. The advantage gained from using small inclination angles in packed columns is due to the increase in gas-liquid interfacial area, enhancing heat and mass transfer. However, negative side-effects of shallow inclination angles, such as larger pressure drops, may negate these improvements.

A unique surface texture pattern on an inclined plate was also investigated. It was found that the addition of vertical ridges, of the same scale as the liquid film thickness, resulted in much larger wetted areas at equivalent Re_l. It is expected that the observed increase is large enough to significantly enhance CO2 absorption within packed columns, especially at very low Re_l.

Future investigations will focus on the addition of reaction kinetics into the models. This will enable the effects of these types of surface textures on CO2 absorption to be measured directly. Studies could also be performed to determine the optimal packing design. Initially, this would focus primarily on optimisation of the surface textures, but could then be extended to include additional effects, such as inclination angles, corrugation angles, gas-liquid flow rates etc.

APPENDIX A
MESH INDEPENDENCE CHECKS

Mesh independence checks were carried out to ensure the results were not effected by the choice of meshes during the investigation. It was observed that the wetted area of the plate was highly dependent upon the flow parameters and therefore, this variable was used as a good indication to mesh dependency. These checks were performed for the smooth plate and textured plate and are detailed below.

A. Smooth Plate

Due to the range of plate inclination angles it was important to ensure grid independent results for all angles. Simulations were run initially with a mesh of 0.6 million cells, increasing the number of cells in subsequent calculations until no significant difference in the solution was observed. Fig. 10 and Fig. 11 plot the specific wetted area against time for $\theta = 60^o$ and $\theta = 30^o$ respectively. It can be seen that there was very
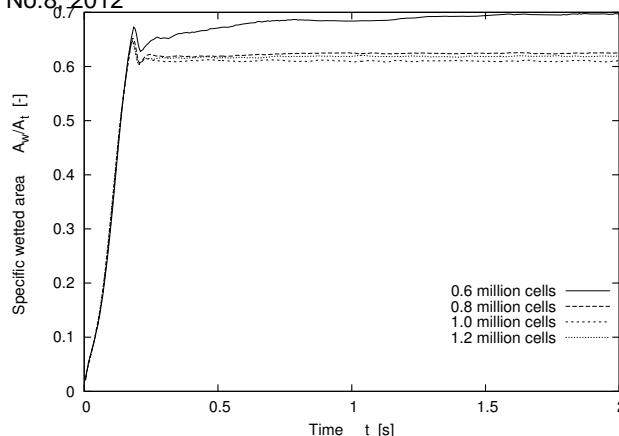

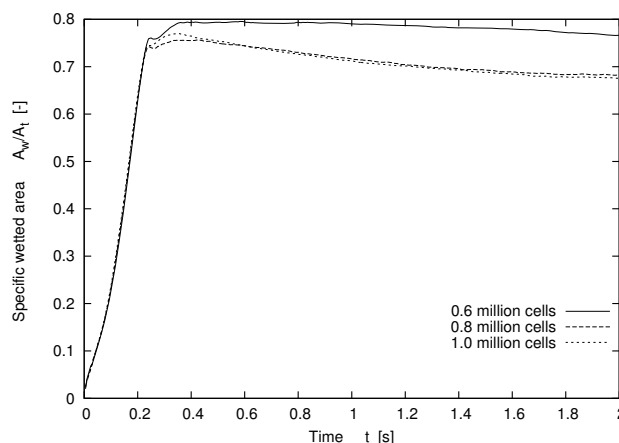Fig. 10.   Specific wetted area against time for smooth plate $\theta = 60^o$

Fig. 11.   Specific wetted area against time for smooth plate $\theta = 30^o$

little difference in the solutions when using meshes of 0.8, 1.0 and 1.2 million cells. It was established that a cell count of 1.0 million cells allowed mesh dependency errors to be minimised for the range of inclination angles, whilst keeping run times to a reasonable level.

B. Textured Plate

Simulations were run initially with approximately 1.4 million cells, increasing the number of cells in subsequent calculations until no significant difference in the solution was observed. Fig. 12 plots the specific wetted area against time for the various computational meshes. It can be seen that the solutions obtained with meshes of 2.0 and 2.5 million cells were consistent with each other. It was decided that a mesh of 2.5 million cells should be used in the investigation, considering the importance of good mesh refinement close to the ridges.
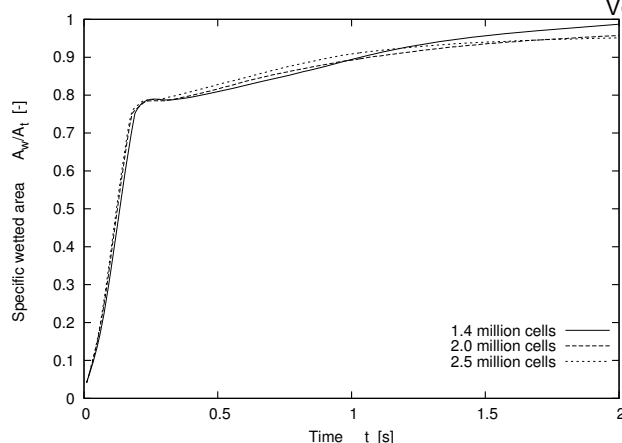
Fig. 12. Specific wetted area against time for textured plate $\theta = 60^o$

at the University of Southampton, in the completion of this work.

REFERENCES

[1] C. D. Ho, H. Chang, H. J. Chen, C. L. Chang, H. H. Li, and Y. Y. Chang, "CFD simulation of the two-phase flow for a falling film microreactor," *International Journal of Heat and Mass Transfer*, vol. 54, pp. 3740–3748, 2011.

[2] P. Chasanis, A. Lautenschleger, and E. Y. Kenig, "Numerical investigation of carbon dioxide absorption in a falling-film micro-contactor," *Chemical Engineering Science*, vol. 65, no. 3, pp. 1125–1133, 2010.

[3] S. Freguia and G. T. Rochelle, "Modeling of CO2 capture by aqueous monoethanolamine," *AIChE Journal*, vol. 49, no. 7, pp. 1676–1686, 2003.

[4] L. Raynal and A. Royon-Lebeaud, "A multi-scale approach for CFD calculations of gas-liquid flow within large size column equipped with structured packing," *Chemical Engineering Science*, vol. 62, no. 24, pp. 7196–7204, 2007.

[5] M. Kohrt, I. Ausner, G. Wozny, and J. U. Repke, "Texture influence on liquid-side mass transfer," *Chemical Engineering Research and Design*, vol. 89, pp. 1405–1413, 2011.

[6] M. R. Khosravi Nikou, M. R. Ehsani, and M. Davazdah Emami, "CFD Simulation of Hydrodynamics, Heat and Mass Transfer Simultaneously in Structured Packing," *International Journal of Chemical Reactor Engineering*, vol. 6, p. A91, 2008.

[7] J. Chen, C. Liu, X. Yuan, and G. Yu, "CFD simulation of flow and mass transfer in structured packing distillation columns," *Chinese Journal of Chemical Engineering*, vol. 17, no. 3, pp. 381–388, 2009.

[8] Y. Y. Xu, S. Paschke, J. U. Repke, J. Q. Yuan, and G. Wozny, "Computational Approach to Characterize the Mass Transfer between the Counter-Current Gas-Liquid Flow," *Chemical Engineering & Technology*, vol. 32, no. 8, pp. 1227–1235, 2009.

[9] Y. Haroun, D. Legendre, and L. Raynal, "Direct numerical simulation of reactive absorption in gas-liquid flow on structured packing using interface capturing method," *Chemical Engineering Science*, vol. 65, no. 1, pp. 351–356, 2010.

[10] B. Szulczewska, I. Zbicinski, and A. Górak, "Liquid flow on structured packing: Cfd simulation and experimental study," *Chemical engineering & technology*, vol. 26, no. 5, pp. 580–584, 2003.

[11] H. Lan, J. Wegener, B. Armaly, and J. Drallmeier, "Developing laminar gravity-driven thin liquid film flow down an inclined plane," *Journal of Fluids Engineering*, vol. 132, p. 081301, 2010.

[12] Y. Y. Xu, S. Paschke, J. U. Repke, J. Q. Yuan, and G. Wozny, "Portraying the Countercurrent Flow on Packings by Three-Dimensional Computational Fluid Dynamics Simulations," *Chemical Engineering & Technology*, vol. 31, no. 10, pp. 1445–1452, 2008.

[13] F. Gu, C. J. Liu, X. G. Yuan, and G. C. Yu, "CFD simulation of liquid film flow on inclined plates," *Chemical engineering & technology*, vol. 27, no. 10, pp. 1099–1104, 2004.

[14] P. Valluri, O. K. Matar, G. F. Hewitt, and M. A. Mendes, "Thin film flow over structured packings at moderate Reynolds numbers," *Chemical engineering science*, vol. 60, no. 7, pp. 1965–1975, 2005.

[15] A. Hoffmann, I. Ausner, J. U. Repke, and G. Wozny, "Fluid dynamics in multiphase distillation processes in packed towers," *Computers & chemical engineering*, vol. 29, no. 6, pp. 1433–1437, 2005.

[16] A. Hoffmann, I. Ausner, J. Repke *et al.*, "Detailed investigation of multiphase (gas-liquid and gas-liquid-liquid) flow behaviour on inclined plates," *Chemical Engineering Research and Design*, vol. 84, no. A2, pp. 147–154, 2006.

[17] Y. Iso and X. Chen, "Flow Transition Behavior of the Wetting Flow Between the Film Flow and Rivulet Flow on an Inclined Wall," *Journal of Fluids Engineering*, vol. 133, p. 091101, 2011.

[18] OpenCFD, *OpenFOAM: The Open Source CFD Toolbox. User Guide Version 2.0.1.* OpenCFD Ltd., Reading UK, 2011.

[19] OpenCFD., *OpenFOAM: The Open Source CFD Toolbox. Programmer's Guide Version 2.0.1.* OpenCFD Ltd., Reading UK, 2011.

[20] C.W. Hirt and B.D. Nichols, "Volume of fluid (VOF) method for the dynamics of free boundaries," *Journal of Computational Physics*, vol. 39, no. 1, pp. 201 – 225, 1981.

[21] H. Rusche, "Computational Fluid Dynamics of Dispersed Two-Phase Flows at High Phase Fractions," Ph.D. dissertation, Imperial College, University of London, Dec 2002.

[22] E. Berberović, N. P. van Hinsberg, S. Jakirlić, I. V. Roisman, and C. Tropea, "Drop impact onto a liquid layer of finite thickness: Dynamics of the cavity evolution," *Physical Review E*, vol. 79, no. 3, p. 036306, 2009.

[23] J. Brackbill, D. Kothe, and C. Zemach, "A continuum method for modeling surface tension," *Journal of Computational Physics*, vol. 100, no. 2, pp. 335–354, 1992.

[24] W. Nusselt, "Die Oberflchenkondensation des Wasserdampfes," *Zeitschrift des Vereines Deutscher Ingenieure*, vol. 60, pp. 541–546 and 569–575, 1916.

[25] C. F. Petre, F. Larachi, I. Iliuta, and B. P. A. Grandjean, "Pressure drop through structured packings: Breakdown into the contributing mechanisms by CFD modeling," *Chemical engineering science*, vol. 58, no. 1, pp. 163–177, 2003.